Implementation of Indirect Field Oriented Control of a 2.2kW Three-Phase Induction Motor Using MATLAB Simulink

Anyanime Tim Umoette
Dept. of Electrical and Electronic Eng
Akwa Ibom State University
Ikot Akpaden, Nigeria
Power Engineering, Durban University of Technology, Durban, South Africa
libertycoast@yahoo.com

Ogbonnaya I. Okoro
Dept. of Electrical and Electronic Eng
Michael Okpara Univ. of Agriculture
Umudike, Nigeria
okoro.ogbonnaya@mouau.edu.ng

Innocent E. Davidson
Dept. of Electrical Power Engineering
Durban University of Technology
Durban, South Africa
ORCID:0000-0002-2336-4136

2021 IEEE AFRICON | 978-1-6654-1984-0/21/$31.00 ©2021 IEEE | DOI: 10.1109/AFRICON51333.2021.9570873

***Abstract*—Speed control of an induction motor using indirect field-oriented control (IFOC) method with space vector pulse width modulation (SVPWM) technique and proportional integral controller is presented and discussed in this paper. A 2.2kW three phase squirrel cage type Induction motor model with field-oriented control was simulated and analyzed using MATLAB/Simulink. The decoupling of the flux and torque producing components, for secondary control was carried out for the actual IFOC of the induction motor drive. The motor performance was analyzed under no-load, variable load, constant speed, and variable speed with load conditions. From the results obtained, the proposed control technique was found to produce satisfactory dynamic response and improved motor performance under these operating conditions.**

Keywords— Induction motor, Speed control, SVPWM, IFOC, MATLAB/Simulink.

I. INTRODUCTION

Induction motors are mostly used in industrial plants due to their high efficiency, ruggedness, low maintenance and reliability. Induction motors deliver high performance in industrial variable speed applications since the development of the vector control method. Indirect field-oriented control (IFOC) is an effective vector control technique of induction motor due to its simplicity of design and implementation [1], [2]. Hence, when a superior performance of induction motor drive is demanded, IFOC is usually used [3]-[4]. In IFOC technique, the flux and torque are decoupled, hence, allowing the two parameters to be controlled independently. Thus, there is an independent control between torque and flux, in q-axis and d-axis respectively.

This enables the induction motor to achieve a dynamic performance similar to a DC drive [6], [7]. IFOC technique for the induction motor provides a standard result by which many other algorithms are compared. Over the years a large number of induction motor research with IFOC strategy have been developed for industry in line with the increasing complexity in industrial operations. For example [8] proposed a modified direct torque control (DTC) which uses the stator to control the torque. In this study, a detailed analysis of vector control concept (both DTC and field-oriented control) is analyzed. Thomas [9] evaluated DTC and FOC on a unique scheme, discrete space vector modulation. The analysis in this study addressed steady-state current, torque ripples, and dynamic response due to a torque step. Vasudevan [10] proposed and experimentally validated geometric sliding mode/limit cycle control, in which three inverter modes, asynchronous, synchronous, and square wave, were analyzed, and focused on industrial applications. Haddoun [11] compared indirect field-oriented control (IFOC) to direct field-oriented control (DFOC). In this study, direct torque control and space vector modulation (DTC-SVM) and direct torque neuro-fuzzy control were evaluated. [12] Presented a special approach on the operation of DFOC, DTC with pulse width modulation (PWM) and DTC-SVM on an electric vehicle. The results show the effectiveness of vector control in electric motor application. Bashke [13] simulated induction motor in real time with a low voltage model and compared the outcome with numerical methods.

An induction motor is a complex and non-linear system that requires more effort in implementing the drive and control system. In this paper, MATLAB/ Simulink software package is used for analyzing speed control of an induction motor using IFOC with Space Vector Pulse Width Modulation (SVPWM), and the industrial variable speed applications are emphasized (like conveyors), where different operations are carried out at a given time intervals at a single operation. The speed control of an induction using IFOC with SVPWM, constitutes the following sub units: flux control, speed control, current control, pulse width modulation unit, inverter and induction motor. These sub-units are built using a Simulink library toolbox based on fundamental equations.

II. INDUCTION MOTOR MODE

The induction motor model equations are generated from d-q axis. An analysis of the Clacke and Park's transformation of the source voltage, for stationary and rotator reference frame respectively are also analyzed. The flux linkages equations on d-q axis are shown in equation (1)-(4). [1]

$$\frac{d\Psi_{qs}}{dt} = w_b[V_{qs} - \frac{w_e}{w_b}\Psi_{ds} + \frac{R_s}{X_{Is}}(\Psi_{mq} - \Psi_{qs})] \quad (1)$$

$$\frac{d\Psi_{ds}}{dt} = w_b[V_{ds} + \frac{w_e}{w_b}\Psi_{qs} + \frac{R_s}{X_{Is}}(\Psi_{md} - \Psi_{ds})] \quad (2)$$

$$\frac{d\Psi_{qr}}{dt} = w_b[V_{qr} - \frac{w_{e-}w_r}{w_b}\Psi_{dr} + \frac{R_r}{X_{Ir}}(\Psi_{mq} - \Psi_{qr})] \quad (3)$$

$$\frac{d\Psi_{dr}}{dt} = w_b[V_{dr} + \frac{w_{e-}w_r}{w_b}\Psi_{qr} + \frac{R_r}{X_{Ir}}(\Psi_{md} - \Psi_{dr})] \quad (4)$$

Where,

$$\Psi_{mq} = X_{m1}[\frac{\Psi_{qs}}{X_{Is}} + \frac{\Psi_{qr}}{X_{Ir}}] \quad (5)$$

$$\Psi_{md} = X_{m1}[\frac{\Psi_{ds}}{X_{Is}} + \frac{\Psi_{dr}}{X_{Ir}}] \quad (6)$$

$$X_{m1} = {}^{1}\Big/\left(\frac{1}{X_m} + \frac{1}{X_{Is}} + \frac{1}{X_{Ir}}\right) \quad (7)$$

The d-axis and q-axis currents are shown in equation (8) – (11), that is, by substituting the flux linkages.

$$i_{qs} = \frac{1}{X_{Is}}(\Psi_{qs} - \Psi_{mq}) \quad (8)$$

$$i_{ds} = \frac{1}{X_{Is}}(\Psi_{ds} - \Psi_{md}) \quad (9)$$

$$i_{qr} = \frac{1}{X_{Ir}}(\Psi_{qr} - \Psi_{mq}) \quad (10)$$

$$i_{dr} = \frac{1}{X_{Ir}}(\Psi_{dr} - \Psi_{md}) \quad (11)$$

The Electromagnetic torque and rotor speed are shown in equation (12) and (13).

$$T_e = \frac{3}{2}\left(\frac{p}{2}\right)\frac{1}{w_b}(\Psi_{ds}i_{qs} - \Psi_{ds}i_{ds}) \quad (12)$$

$$w_r = \int \frac{p}{2J}(T_e - T_L) \quad (13)$$

Where p is the number of poles, ,J is the moment of initia $\left({}^{kg}/_{m^2}\right)$,

For squirrel cage induction motor, the motor voltages V_{qr} and V_{dr} bars are shorted. Having derived the speed and torque equations in term of d-q flux linkages and currents of the stator, the same is applicable to the voltages that is applied to the stator. In a balanced condition, the three-phase stator voltages of an induction motor can be expressed as:

$$V_a = \sqrt{2}V_{rms}\sin(wt) \quad (14)$$

$$V_b = \sqrt{2}V_{rms}\sin\left(wt - \frac{2\pi}{3}\right) \quad (15)$$

$$V_b = \sqrt{2}V_{rms}\sin\left(wt + \frac{2\pi}{3}\right) \quad (16)$$

A. Clarke Transformation

The Clarke transformation converts a three-phase system into a two-phase system (that is, to stationary reference frame). Taking the voltages in equation (14), (15), and (16), equation (7) and (8) are generated.

Equation (19) represents the Clarke transformation in matric form. Figure 1 represents the Simulink model of the Clarke transformation.

$$V_\alpha = \frac{2}{3}V_a + \frac{1}{3}V_b - \frac{1}{3}V_c \quad (17)$$

$$V_\beta = \frac{1}{\sqrt{3}}V_b - \frac{1}{\sqrt{3}}V_c \quad (18)$$

$$\begin{bmatrix}V_\alpha \\ V_\alpha\end{bmatrix} = \frac{2}{3}\begin{bmatrix}1 & {}^1/_2 & -{}^1/_2 \\ 0 & {}^{\sqrt{3}}/_2 & -{}^{\sqrt{3}}/_2\end{bmatrix}\begin{bmatrix}V_a \\ V_b \\ V_c\end{bmatrix} \quad (19)$$

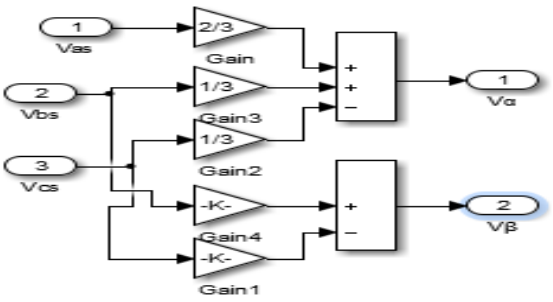

Fig. 1. Simulink model of Clarke transformation of three-phase currents

B. Park Transformation

The equations from the clarke transformation is in the stationary reference frame in $\alpha\beta$ axis, and park transformation is further use to transform the equations to a rotating reference frame in direct and quadrature axis. This can be shown in equation (20).

$$\begin{bmatrix}V_d \\ V_q\end{bmatrix} = \begin{bmatrix}\cos\theta & \sin\theta \\ -\sin\theta & \cos\theta\end{bmatrix}\begin{bmatrix}V_\alpha \\ V_\beta\end{bmatrix} \quad (20)$$

The stator and rotor currents in three-phase system are calculated as shown in equation (21) and (22), and the Simulink model for park transformation is shown in figure 2.

$$\begin{bmatrix}i_\alpha \\ i_\beta\end{bmatrix} = \begin{bmatrix}\cos\theta & -\sin\theta \\ \sin\theta & \cos\theta\end{bmatrix}\begin{bmatrix}i_d \\ i_q\end{bmatrix} \quad (21)$$

$$\begin{bmatrix}i_a \\ i_b \\ i_c\end{bmatrix} = \frac{2}{3}\begin{bmatrix}1 & 0 \\ -{}^1/_2 & -{}^{\sqrt{3}}/_2 \\ -{}^1/_2 & {}^{\sqrt{3}}/_2\end{bmatrix}\begin{bmatrix}i_a \\ i_\beta\end{bmatrix} \quad (22)$$

Indirect Field Oriented Control (IFOC)

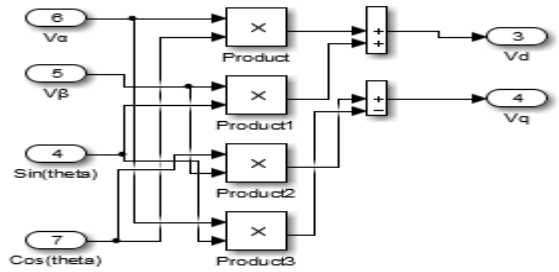

Fig. 2. Simulink model of Park transformation of $\alpha\beta$ axis currents

The IFOC principle was introduced by Blaschke [14] where similar DC motor characteristics is created in an induction motor derive. This is a fundamental concept of vector control (FOC) where an induction motor is operated like a separately excited DC motor. The FOC technique is widely used when dealing with complex industrial processes. Under this concept, the motor flux and torque are decoupled and control separately. Decoupling of an induction motor is not so simple because of the coupling effect between the torque and fluxes, whose orientations (in terms of degree between them) vary according to the operating conditions of the motor. DC machine-similar performance can be obtain in

an induction motor by separating and controlling independently the field and armature fluxes in the motor by orienting the stator current with respect to the rotor flux [15], [16]. There are two ways of achieving FOC, they are: direct field oriented control (DFOC) and indirect field oriented control (IFOC). In DFOC, the rotor position is realized by a senor, however, the inclusion of the sensor complicates the system and also make the technique uneconomical [17]. While in IFOC, the position of rotor flux is predicted from the model of induction motor (block diagram shown in figure 4). From the phasor (figure 3) diagram, is it shown that for decoupling control, the flux producing component is on direct axis, while the torque component on the quadrature- axis . Main limitation of IFOC is that it sensitive to motor parameters if an incorrect value of rotor time constant is provided, it can cause a misalignment between the stator current and rotor flux thus, reduces the system performance.

For the decoupling of flux and torque producing components, the rotor equations can be written as

$$\frac{d\psi_{dr}}{dt} + R_r i_{dr} - (\omega_e - \omega_r)\psi_{qr} = 0 \quad (23)$$

$$\frac{d\psi_{qr}}{dt} + R_r i_{dr} - (\omega_e - \omega_r)\psi_{dr} = 0 \quad (24)$$

The rotor flux linkage expressions are

$$\psi_{dr} = L_r i_{dr} + L_m i_{ds} \quad (25)$$

$$\psi_{qr} = L_r i_{qr} + L_m i_{qs} \quad (26)$$

From this expression, we can write

$$i_{dr} = \frac{1}{L_r}\psi_{dr} - \frac{L_m}{L_r} i_{ds} \quad (27)$$

$$i_{qr} = \frac{1}{L_r}\psi_{qr} - \frac{L_m}{L_r} i_{qs} \quad (28)$$

Putting (5) and (6) in (1) and (2), we have,

$$\frac{d\psi_{dr}}{dt} + R_r \frac{1}{L_r}\psi_{dr} - \frac{L_m}{L_r} R_r i_{ds} - (\omega_{sr})\psi_{qr} = 0 \quad (29)$$

$$\frac{d\psi_{qr}}{dt} + R_r \frac{1}{L_r}\psi_{qr} - \frac{L_m}{L_r} R_r i_{qs} - (\omega_{sr})\psi_{dr} = 0 \quad (30)$$

$$\omega_{sr} = \omega_e - \omega_r \quad (31)$$

For decoupling control

$$\psi_{qr} = 0 \quad (32)$$

$$\frac{d\psi_{qr}}{dt} = 0 \quad (33)$$

Substituting these equations in (7) and (8). We have

$$\frac{L_r}{R_r}\frac{d\psi_r}{dt} + \psi_r = L_m i_{ds} \quad (34)$$

$$\omega_{sr} = \frac{L_m}{\psi_r}\frac{R_r}{L_r} i_{qs} \quad (35)$$

$$Te = \frac{3}{2}\left(\frac{P}{2}\right)\frac{L_m}{L_r}\psi_r i_{qs} \quad (36)$$

From the block diagram in figure 4, signal ω_{sr} obtained is added with rotor speed signal ω_r to generate frequency signal ω_e, Rotor flux angle θ_e for coordinate transformation is obtained from equation (37)

$$\theta_e = \int(\omega_r + \omega_{sr})dt \quad (37)$$

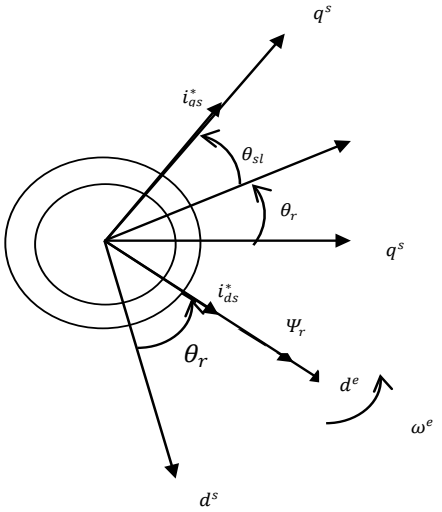

Fig. 3. Phasor diagram of IFOC of an Induction motor.

III. SPACE VECTOR PULSE WIDTH MODULATION

Space Vector Pulse Width Modulation (SVPWM) technique is a preferred technique for Pulse Width Modulation voltage source inverter since it gives an output with less harmonic distortion. In this technique, phase voltages are represented as space vector model and the inverter is switching between two adjacent active vectors and a zero vectors during one switching period [18]. There are eight possible states, which are associated with a reference vector, and for possible of generating a rotating field, and the inverter has to be switched in six of the eight states [19]. The other two states are zero vectors. From figure 6, the angle between any two vectors is 60°. the notation that describes the states of the three phase inverter (shown in figure 6) and the corresponding voltages is recorded in Table 1, this depends on the on and off state of the transistor. For example, the state when transistors T1, T4, T5 are on and T2, T3, T6 are off can be represented with the notation (+ - +). The line –to – neutral voltages can be converted into a space vector U_s from equation (38)

$$U_s = V_{an}(t)e^{j0} + V_{bn}(t)e^{j\frac{2}{3}} + V_{cn}(t)e^{-j\frac{2}{3}} \quad (38)$$

Where the components are of angles $\left(0, \frac{-2\pi}{3}, \frac{2\pi}{3}\right)$

The reference voltage vector (U_s) is sampled with the fixed clock frequency $f_s = 1/T_s$, if reference voltage falls at section one from figure 2, taking $U_0 = V_{1,} U_{60} = V_{2,} U_s = V_{ref,}$, then:

$$V_{ref} = \frac{t_1}{T_s}(V_1) + \frac{t_2}{T_s}(V_2) \quad (39)$$

As the amplitude of $V_{1,}$ and $V_{2,}$ are equal to $2Vdc/3$, hence

$$t_1 = \sqrt{3}T_s \frac{V_{ref}}{Vdc}\sin(60 - \alpha) \quad (40)$$

$$t_2 = \sqrt{3}T_s \frac{V_{ref}}{Vdc}\sin\alpha \quad (41)$$

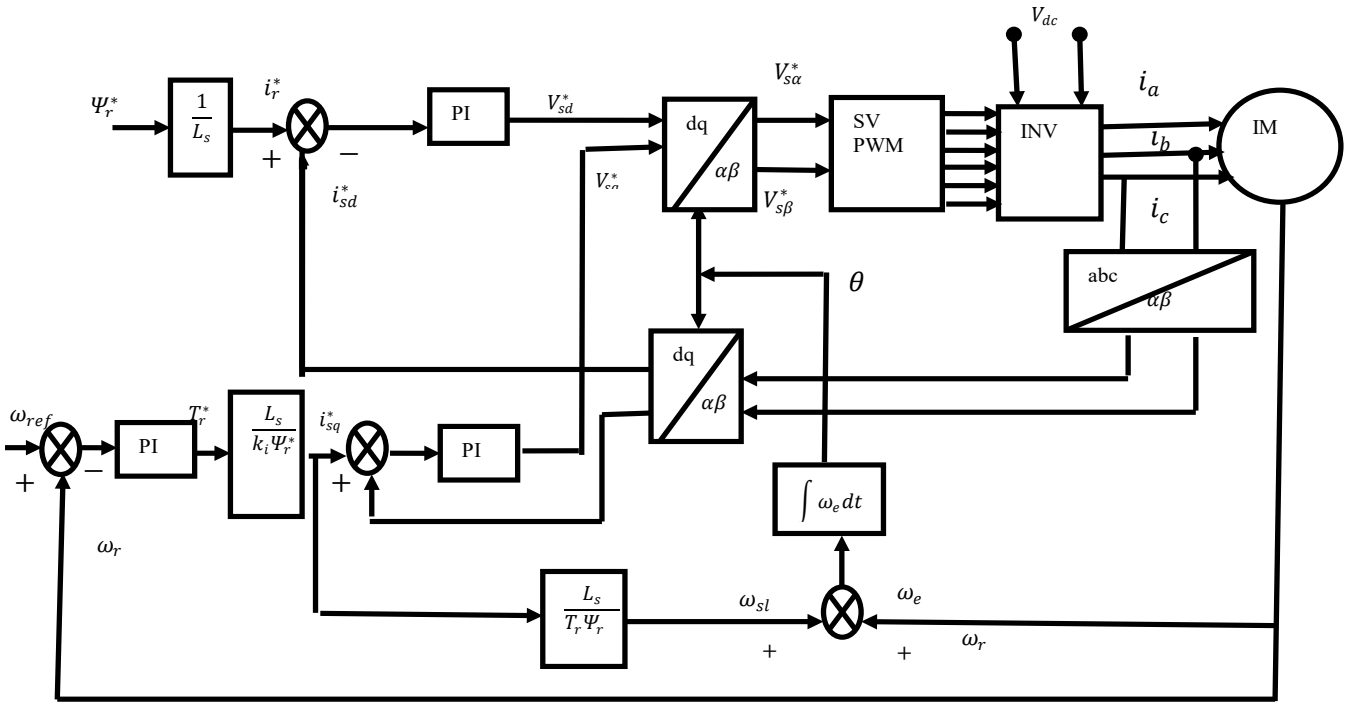

Fig. 4. Block diagram of IFOC of an Induction motor.

IV. Proportional Integral Controller

The proportional Integral controllers are use as the main controller in this model, for the speed, flux and torque control. As the difference between the reference value and actual value grows, the *P* term increases relatively to provide correction. The Integral (I) term of the controller is used to eliminate small steady state errors. The Simulink model of the PI speed controller is shown in Figure 5. And the analysis of the output value of the controller is given in equation (4) to (7)

$$output(t) = K_P e(t) + K_i \int_0^1 e(\tau)d\tau \quad (42)$$

$e(t)$ = Set Reference Value – Actual Calculated Value

$$e(t) = \omega_{ref} - \omega_m(t) \quad (43)$$

$$T_{ref}(t) = T_{ref}(t-1) + K_i[e(t) - e(t-1)] + K_i e(t) \quad (44)$$

Where K_P is proportional gain and K_i is integral gain. Figure 13 represents the implementation of the PI controller

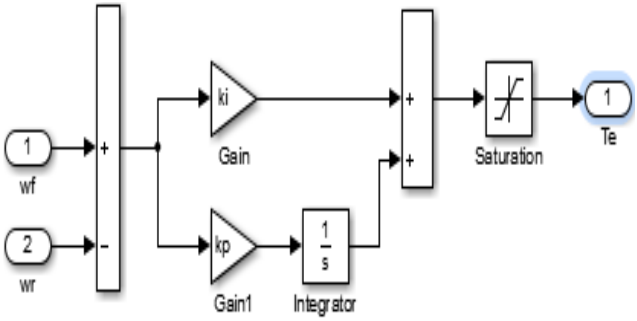

Fig. 5. Simulink implementation of PI controller

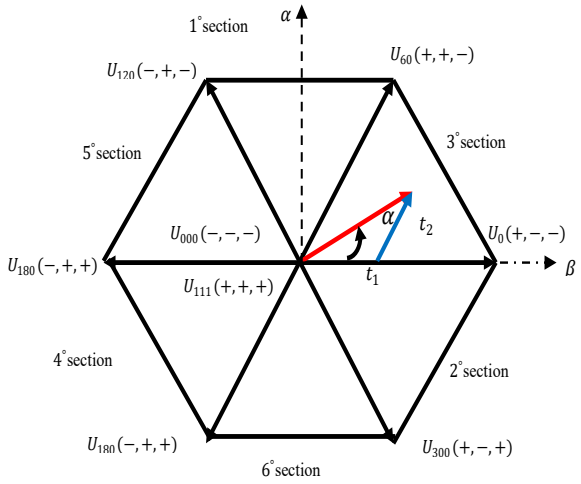

Fig. 6. Representation of an inverter state in reference frame

Table 1: Summary of Switching State

State C	On Device	Va	Vb	Vc	Space voltage vector
0	T2,T4,T6	0	0	0	$0_{000}(-,-,-,)$
1	T1,T4,T6	$2Vdc/3$	$-Vdc/3$	$-Vdc/3$	$0_{000}(+,-,-,)$
2	T1,T3,T6	$Vdc/3$	$Vdc/3$	$-2Vdc/3$	$0_{60}(+,+,-,)$
3	T3,T2,T6	$-Vdc/3$	$2Vdc/3$	$-Vdc/3$	$0_{120}(-,+,-,)$
4	T2,T3,T5	$-2Vdc/3$	$Vdc/3$	$Vdc/3$	$0_{180}(-,+,+,)$
5	T2,T4,T6	$-Vdc/3$	$-Vdc/3$	$2Vdc/3$	$0_{240}(-,-,+,)$
6	T1,T4,T5	$Vdc/3$	$-2Vdc/3$	$Vdc/3$	$0_{300}(+,-,+,)$
7	T1,T3,T5	0	0	0	$0_{111}(+,+,+,)$

V. Simulation Results and Analysis

The IFOC strategy is shown in Fig.4, the simulation is done by using the Simulink toolbox of MATLAB. The parameters of the tested motor are listed in table 1.The proportional integral controller was used with proportional gain and integral gain of 37 and 89 respectively. For a better understanding of the performance of an induction motor based on Space Vector Pulse Width Modulation under IFOC method, different operational modes have been tested, these include: no-load at command speed of 100rad/sec, under the constant load at different speed values, constant speed at different load values, and under the variable command speed load values. The detailed explanations of the Simulation results are given the subsequent sections.

Table II: Summary of Switching State

Motor parameters	specification
voltage	380
Power	2.2kW
Frequency	50Hz
Rotor Resistance	0.328Ω
Stator Resistance	0.097Ω
Rotor Inductance	0.891×10^{-3}
Stator Inductance	0.891×10^{-3}
Mutual Inductance	0.0447H
Pole	4
Initial	$1.092 Kgm^2$
Rated speed	1435RPM

A. No Load

The simulation results of the on load operation representing the torque and Speed are shown in figure 7, and figure 8 respectively, the speed and torque waveform stabilizes and settle at 0.8 sec. The results of the speed (figure8) indicates a dynamic response at no load, where the operation continue at the command speed of 100 rad/sec after the time rise and settling time of 0.8seconds with minimum overshoots.

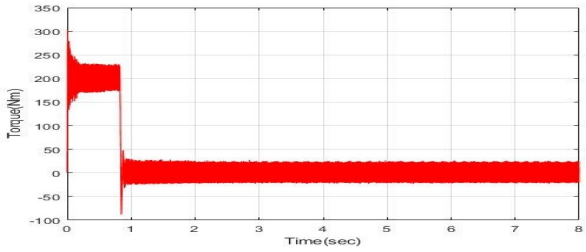

Fig. 7. Electromagnetic torque at no load

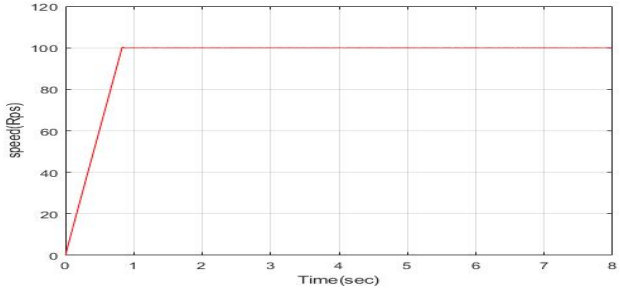

Fig. 8. Rotor Speed at no load

B. Step Change in Load Torque at Constant Speed

The responses of the motor on step change in load torque at constant speed are shown in figure (9) and (10) representing torque and speed respectively. Loads of 50Nm, 200Nm, and 60Nm were introduced at the time range of 0 second to 3 seconds, 3 second to 5 second and 5 second to 8 second respectively. The main advantage of indirect field oriented control is shown in figure (10) where the speed of the motor remains constant even at load change. Also it can be seen that the dynamic torque response is fast for this level of operation

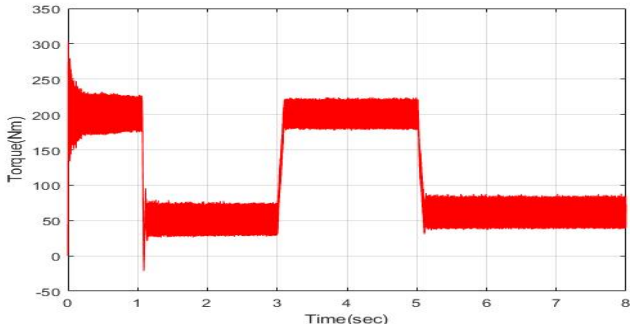

Fig. 9. Electromagnetic torque at Variable load

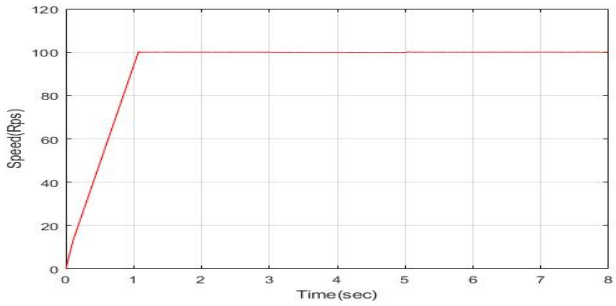

Fig. 10. Speed at Variable load

C. Variable Speed and Load Operation

The responses of the motor on variable speed and load operation are shown in figure (11) and (12) representing torque and rotor speed. This is a typical variable speed application, where within a system's singular operation, different speeds and loads are demanded. In this operation, load of 50Nm, 100Nm, 200Nm and 60Nm were introduced at 0 seconds to 3 seconds, 3 seconds to 4 seconds, 4 seconds to 5 second and 5 seconds to 8 seconds for the command speed of 50rps, 100rps and 60rps respectively. The simulation results shows the performance of this motor at variable speed/load operation. The simulation results show a good response to the command speed and load values, which shows that, IFOC method using PI controller has provided an improve running operations of the motor at this condition.

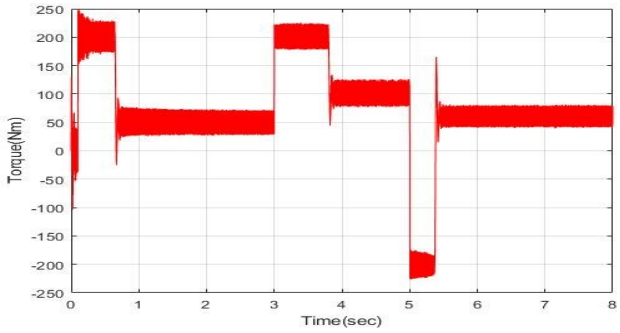

Fig.11. Electromagnetic torque at Variable load and speed

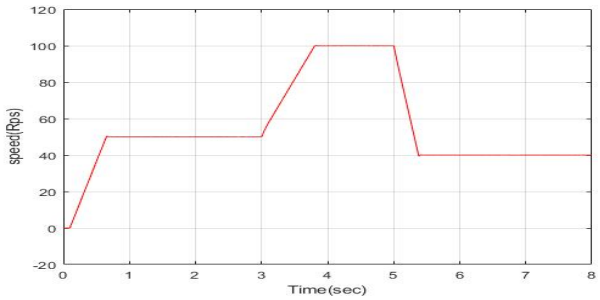

Fig.12. Rotor speed at Variable load and speed

VI. Conclusion

This paper has presented the indirect field oriented control (IFOC) of an induction motor using space vector pulse width modulation technique. In this technique, the flux and torque components were decoupled and controlled separately in d-axis and q- axis respectively. The simulation was carried out in MATLAB/Simulink, and the simulation results verify the proposed control technique. The dynamic requirement of indirect field oriented control is achieved by applying PI controller in the model. The simulation results of IFOC shown are: rotor speed, and electromagnetic torque, and these results represent the motor performance under different conditions of load and speed variation. The operational performance was analyzed under: no-load, constant speed with variable load and variable speed and load condition. Finally, from the results, the model has reduced the initial ripples that normally occur in the torque and speed waveform of an induction motor, and also maintain the desire speed despise load variations. The simulation results show that the proposed control technique improves the performance of the motor under the aforementioned operating conditions.

Acknowledgement

This work is supported by the Centre of Excellence in Smart Grid Research, Durban University of Technology, Durban, South Africa

References

[1]. B. Bose, Power Electronics and AC Drives. Englewood Cliffs, NJ: Prentice-Hall, 1986

[2]. K. Bose, Power Electronic and Motor Drives. California, USA: Elsevier, 2006.

[3]. X. Longya, and T. Y. Brian , "Fuzzy Logic Enhanceed Speed Control of an Indirect Field Oriented Induction Machine drive," *IEEE Transaction on Power Electronics,* vol. 12, no. 5, 1997.

[4]. M. Abdelkader , B. Yessema and M. Chebre, "Speed Control of Induction Motor Using Genetic Algorithm based PI Controller," Acta Polytechnica Hungarica, pp. 141-153, 2011.

[5]. M. Mannan.T. Murata, J.Tamura,T.suchiya ."Indirect Field Oriented Control For High Performance Induction Motor Drives Using Space Vector Modulation With Consideration Of CoreLoss", *IEEE Power Electronics Specialist Conference* 2003, Vol 3, pp 1449-1454.

[6]. T. Murata, T. Tsuchiya and I. Takeda, "Vector Control for Induction Machine on the Application of Optimal Control Theory," *IEEE Trans on Industrial Electronics*, vol. 37, no. 4, p p. 283-290, 1990.

[7]. T. G. Habetler., "Direct torque control of induction machines using space vector modulation," *IEEE Transactions on Industry Applications*., vol. 28, pp. 1045–1053, Sept./Oct. 1992.

[8]. D. Casadei, F. Profumo, G. Serra, and A. Tani, "FOC and DTC: Two Variable Schemes for Induction Motors Torque Control," *IEEE Trans. Power Electronics*, vol. 17, no. 5, pp. 779 - 787, Sept. 2002.

[9]. J. L. Thomas, "Future practical developments in vector control principles," in IEE Colloquium Vector Control, 1998, pp. 4/1 - 4/8.

[10]. M. Vasudevan and R. Arumugam, "Different viable torque control schemes of induction motor for electric propulsion systems," in Conf. Rec., *IEEE Industry Applications Soc. Annual Meeting*, 2004, pp. 2728 - 2737.

[11]. Haddoun, M. E. H. Benbouzid, D.Diallo, R. Abdessemed, J. Ghouili, and K. Srairi, "Comparative analysis of control techniques for efficiency improvement in elective vehicles," in *Proc. IEEE Vehicle Power Propulsion Conf.*, 2007, pp. 629 – 634

[12]. A. Ingalalli and J. V. V. N. Bapiraju, "Analytical model for real-time simulation of low voltage induction motor drive," in 2017 *IEEE International Electric Machines and Drives Conference* (IEMDC), Miami, FL, 2017

[13]. F.Blashke," The principle of field orientation as applied to the new transvector closed loop control system for rotating field machines", *Siemens Review*, Vol 39,no.5,pp 217-220,May 1972

[14]. C.B.Jacobina, J. Bione Fo, F. Salvadori, A.M.N.Lima and L.A.S. Riberio, "A Simple Indirect Field Oriented Control of Induction Machines witout Speed Measurement". *IEEE Transactions on Industry Applications*.2000 pp.1809-1813.

[15]. J. Holtz and J. Quan, " Sensorless vector control of induction motors at very low speed using a nonlinear inverter model and parameter identification", *IEEE Trans. on Industry Applications*, vol. 38, Issue: 4, July-Aug 2002.

[16]. H. S. Rajamani and R. A. McMahon, "Induction motor drives for domestic appliances," *IEEE Transactions on Industrial Applications,* vol. 3, No. 3, pp. 21-26, 1997.

[17]. H. W. Van Der Brock, H. C. Skudelny and G. V. Stanke, "Analysis and Realization of a Pulse Width Modulator Based on Voltage Space Vectors," *IEEE Trans on Industry Applications*, vol. 24, no. 1, pp.142- 150,1988

[18]. S.A Mir and E. Elbuluk, "Fuzzy controller for Inverter fed Induction Machines", *IEEE Transactions on Industry Applications, v*ol. 30, Issue 1, pp. 78-84, Jan 1994

[19]. L. Zicheng,, LYongdong , and Z. Zheng. "A review of drive techniques for multiphase machines." CES Transactions on Electrical Machines and Systems 2, no. 2 (2018): 243-251.